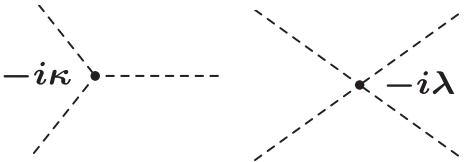

Figure 2.1 Three- and four-point interactions of a Hermitian scalar field ϕ. The factor is the coefficient of $\phi^n/n!$ in $i\mathcal{L}$, as described in Appendix B.

002x001.eps

Figure 2.2 Diagrams with additional factors of 1/2! (left) and 1/3! (right), required because not all of the $(4!)^2$ ways of associating the four fields at each vertex with four lines lead to distinct diagrams.

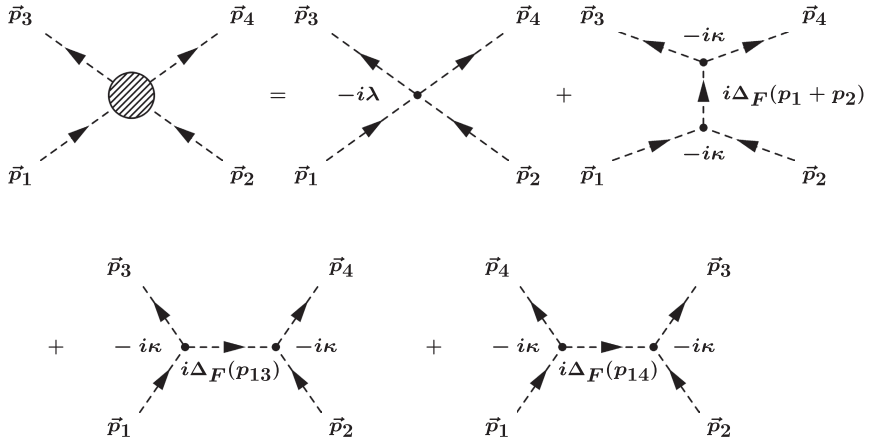

Figure 2.3 Tree level diagrams for $M_{fi} = \langle \vec{p}_3\, \vec{p}_4 | M | \vec{p}_1 \vec{p}_2 \rangle$ for a Hermitian scalar field. The arrows label the directions of momentum flow, and $p_{ij} \equiv p_i - p_j$. The arrangement of lines in the last diagram is modied to allow the diagram to be drawn without crossing lines.

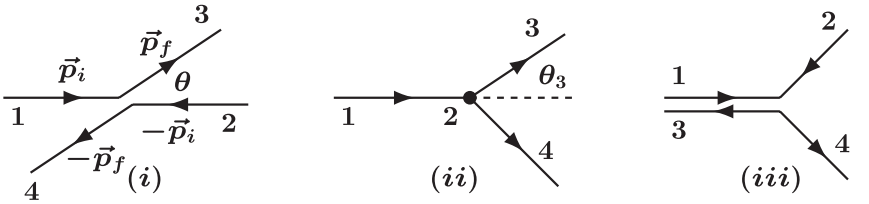

Figure 2.4 Scattering kinematics in (i) the center of mass, (ii) the lab, and (iii) the Breit frames.

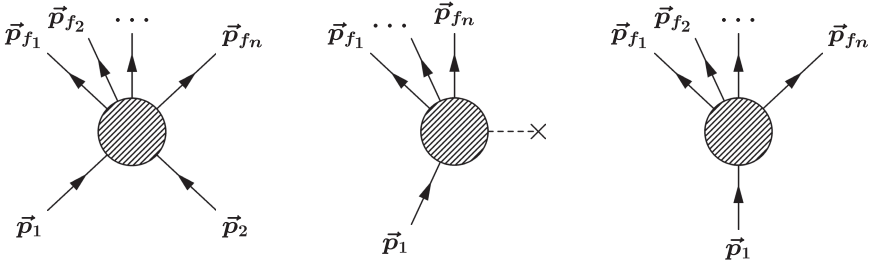

Figure 2.5 The $2 \to n$ scattering process $p_1 p_2 \to pf_1 \cdots pf_n$ (left); $1 \to n$ scattering $p_1 \to pf_1 \cdots pf_n$ from a potential, represented by a cross (middle); and the $1 \to n$ decay process $p_1 \to pf_1 \cdots pf_n$ (right).

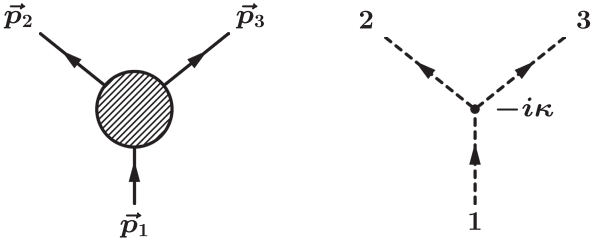

Figure 2.6 The two-body decay of the spin-0 scalar 1 into 2 + 3, and the associated Feynman diagram corresponding to (2.84).

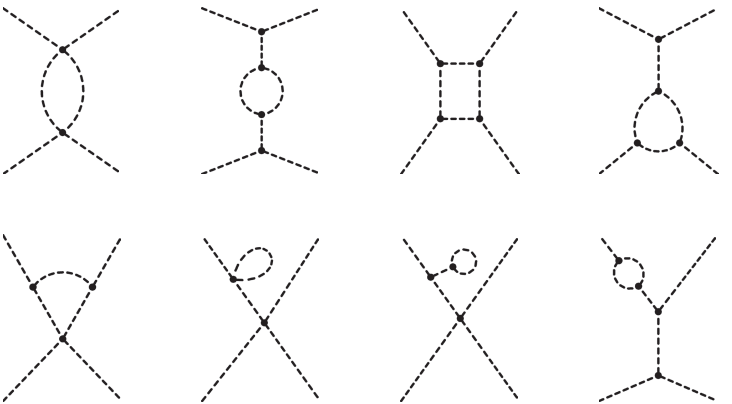

Figure 2.7 Examples of one-loop diagrams contributing to the process $p_1 p_2 \to p_3 p4$.

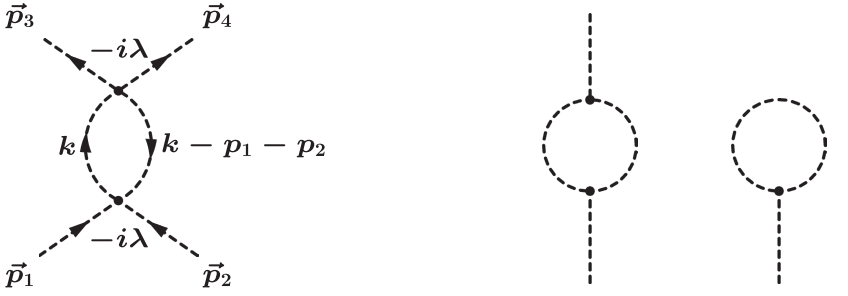

Figure 2.8 Left: A typical one-loop diagram, with the momenta flowing through each line labeled. Right: Divergent (sub)diagrams in the super-renormalizable ϕ^3 theory. The second (*tadpole*) diagram contributes to the d_1 term in (2.21) and must be included in the field redenition that eliminates it.

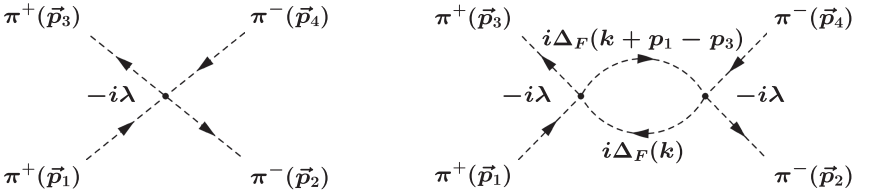

Figure 2.9 Left: Tree-level diagram for $\pi^+(\vec{p}_1)\pi^-(\vec{p}_2) \to \pi^+(\vec{p}_3)\pi^-(\vec{p}_4)$, where $\vec{p}_{1,2}$ ($\vec{p}_{3,4}$) are the physical initial (final) momenta. Right: An example of a one-loop diagram. $\Delta_F(k)$ is dened in (2.29).

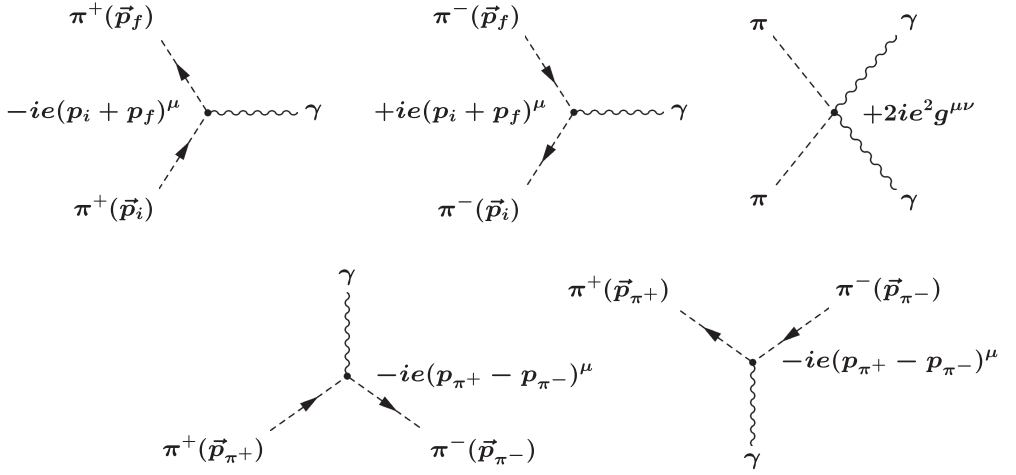

Figure 2.10 Vertices involving charged pions and one or two photons. In the onephoton diagrams the initial pions enter from the bottom and the final leave from the top. Antiparticle (p^-) vertices are obtained from particle ones by twisting the lines and replacing p by $\bar{p} \equiv -p$, where p is the physical four-momentum and $\bar{p}$ follows the direction of the arrow. The wavy lines represent photons.

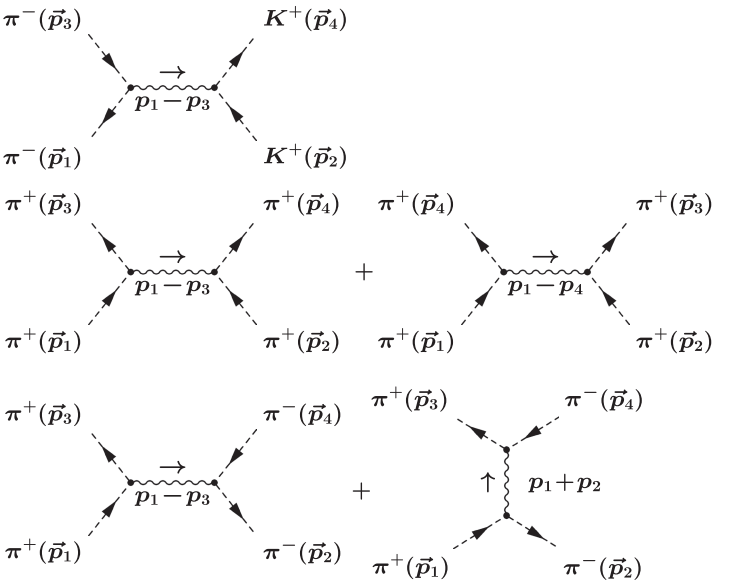

Figure 2.11 Feynman diagrams for $\pi^- K^+ \to \pi^- K^+$(top), $\pi^+\pi^+ \to \pi^+\pi^+$ (middle), and $\pi^+\pi^- \to \pi^+\pi^-$ (bottom).

002x011.eps

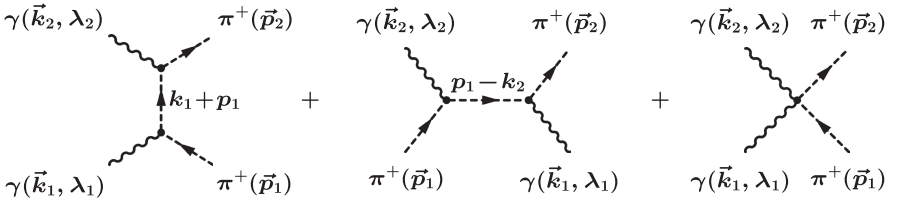

Figure 2.12 Diagrams for pion Compton scattering. The third (seagull) diagram is required by gauge invariance.

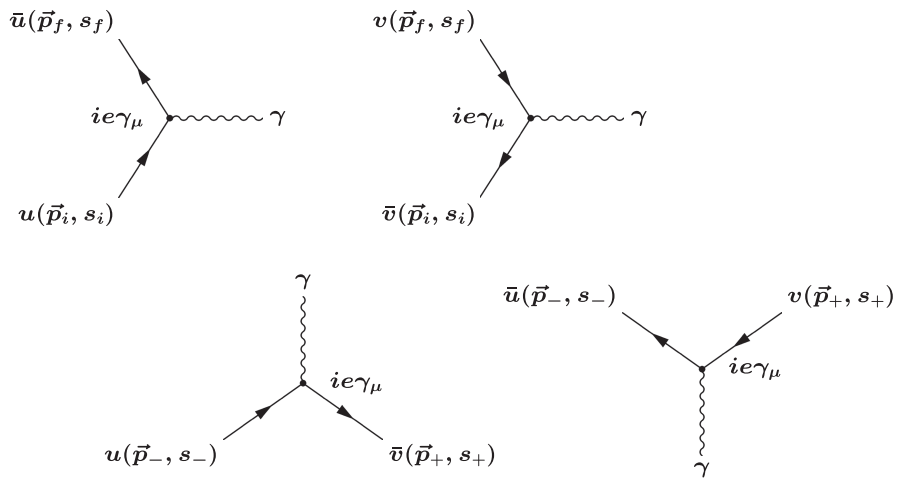

Figure 2.13 Vertices involving the interactions of $e^{\pm}$ with a photon. The initial fermions enter from the bottom and the final leave from the top. ± refer to a positron or electron, respectively. Note the crossing symmetry, i.e., up to an overall sign the amplitude for an initial positron can be obtained from that for a final electron except $\overline{u} \to \overline{v}$, always using the physical momentum and spin, and similarly for the relation of a final positron and initial electron.

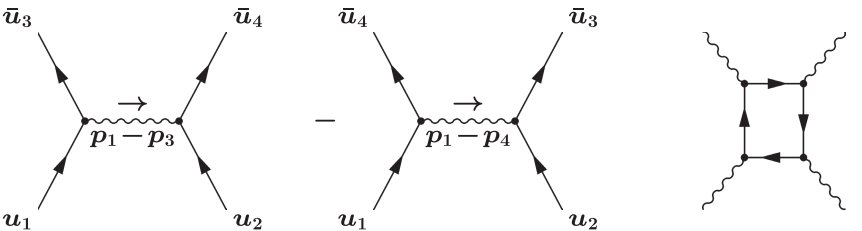

Figure 2.14 Left and center: relative minus signs between diagrams involving exchanged fermion lines, with $u_i \equiv u(\vec{p}_i, s_i)$. Right: a closed loop diagram, with an extra factor of –1.

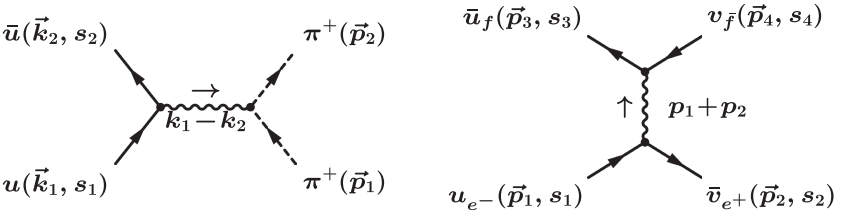

Figure 2.15 Left: lowest order diagram for $e^-(\vec{k}_1)\pi^+(\vec{p}_1) \to e^-(\vec{k}_2)\pi^+(\vec{p}_2)$. Right: diagram for $e^-(\vec{p}_1)e^+(\vec{p}_2) \to f(\vec{p}_3)\overline{f}(\vec{p}_4)$, where $f \neq e^{\pm}$.

002x015.eps

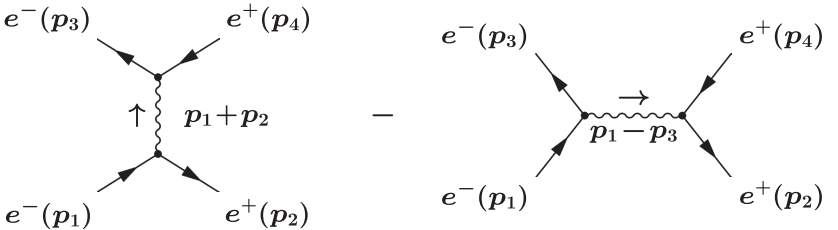

Figure 2.16 Feynman diagrams for $e^-(\vec{p}_1)e^+(\vec{p}_2) \to e^-(\vec{p}_3)e^+(\vec{p}_4)$. The relative minus sign between the two diagrams is independent of state conventions.

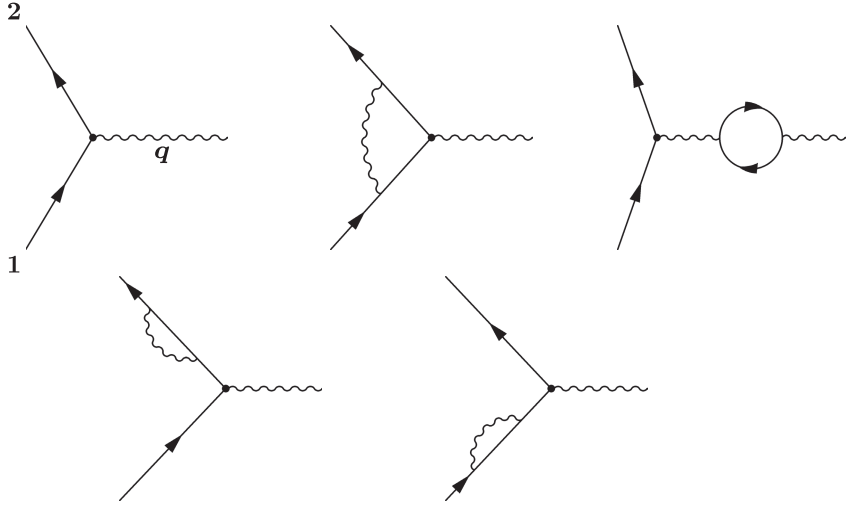

Figure 2.17 Electron-photon vertex (top left), and one-loop corrections, corresponding to the vertex correction(top middle), the vacuum polarization (or photon self-energy) correction (top right), and electron self-energy corrections (bottom).

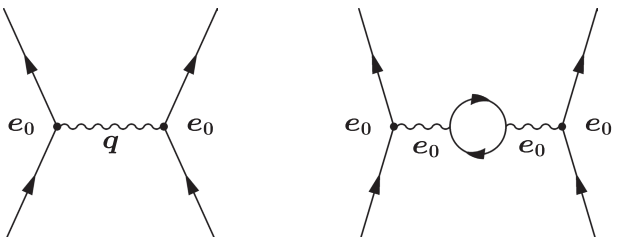

Figure 2.18 One photon exchange and one-loop vacuum polarization "bubble."

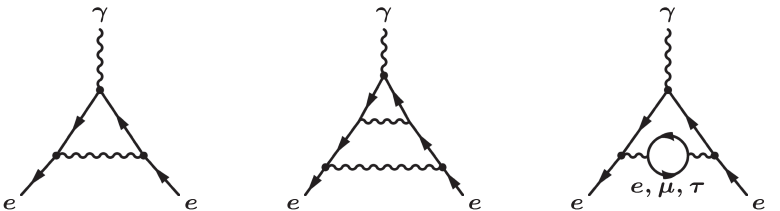

Figure 2.19 One-loop and typical two-loop diagrams contributing to the anomalous magnetic moment of the electron.

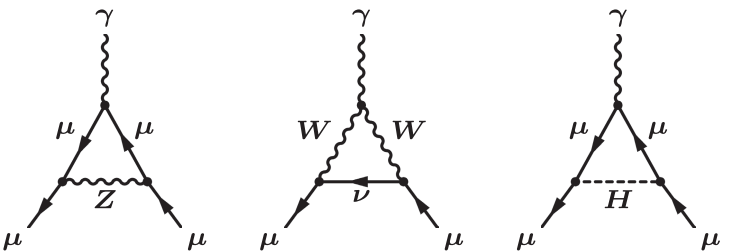

Figure 2.20 One-loop electroweak contributions to $a_\mu = (g_\mu - 2)/2$.

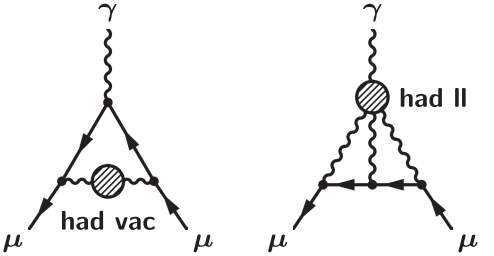

Figure 2.21 Two-loop hadronic vacuum polarization (left) and hadronic light by light (right) diagrams.The shaded blobs represent hadronic states.

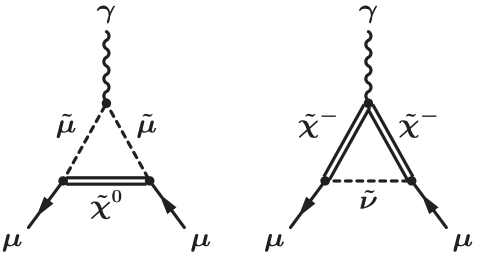

Figure 2.22 New contributions to α_μ in the supersymmetric extension of the SM. $\tilde{\mu}$ and $\tilde{\nu}$ are the spin-0 superpartners of the μ and ν, while $\tilde{\chi}^{\pm,0}$ are spin $-\frac{1}{2}$ superpartners of the electroweak gauge bosons and Higgs fields.

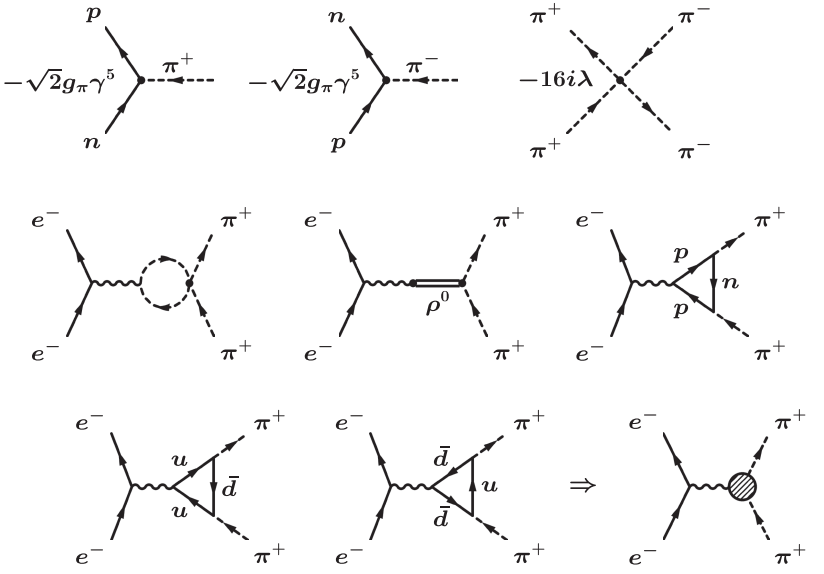

Figure 2.23 Top: interaction vertices described by (2.381). Middle: representative strong interaction diagrams contributing to $\langle \pi^+ | J_Q^\mu | \pi^+ \rangle$ involving nucleons, pions, and the ρ^0 resonance. Bottom left: diagrams in the quark model description in which the π^+ is a $u\bar{d}$ bound state. Bottom right: parametrization of the strong interaction effects by a form factor, represented by a shaded circle.

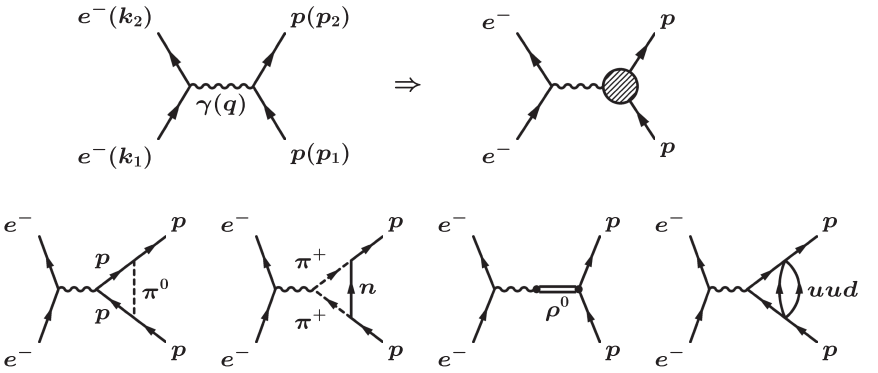

Figure 2.24 Top: tree-level amplitude for for a point proton and with proton form factors (shaded circle). Bottom: representative strong interaction corrections in terms of virtual hadrons (three left diagrams) or in terms of quark constituents (right).

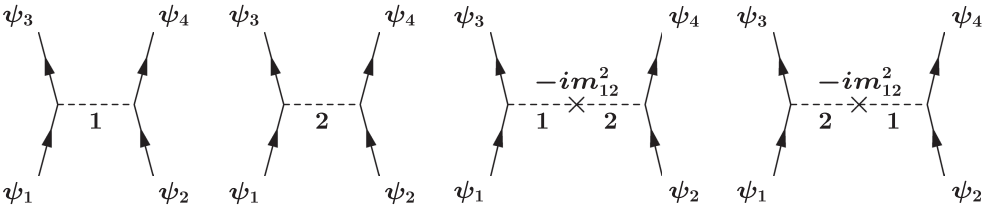

Figure 2.25 t-channel diagrams for $\psi_1\psi_2 \to \psi_3\psi_4$, treating the m_{12}^2 term in (2.410) as a perturbative mass insertion. There are additional u channel diagrams with $(3 \leftrightarrow 4)$.